Chemistry–A European Journal
Research Article
doi.org/10.1002/chem.202103984
Chemistry Europe
European Chemical Societies Publishing
www.chemeurj.org

Binding Interactions in Copper, Silver and Gold π-Complexes

Jaya Mehara[+],[a] Brandon T. Watson[+],[b] Anurag Noonikara-Poyil,[b] Adway O. Zacharias,[b] Jana Roithová,*[a] and H. V. Rasika Dias*[b]

Abstract: The copper(I), silver(I), and gold(I) metals bind π-ligands by σ-bonding and π-back bonding interactions. These interactions were investigated using bidentate ancillary ligands with electron donating and withdrawing substituents. The π-ligands span from ethylene to larger terminal and internal alkenes and alkynes. Results of X-ray crystallography, NMR, and IR spectroscopy and gas phase experiments show that the binding energies increase in the order Ag < Cu < Au and the binding energies are slightly higher for alkynes than for alkenes. Modulation of the electron density at the metal using substituents on the ancillary ligands shows that the π-back bonding interaction plays a dominant role for the binding in the copper and gold complexes.

Introduction

Coinage metals (Cu, Ag, and Au) play critical roles in chemical transformations of small unsaturated hydrocarbons such as olefins and alkynes.[1] For example, copper(I) salts and complexes are often employed as catalysts in azide-alkyne cycloadditions,[2] cyclopropanation of alkenes,[3] and cyclopropenation of alkynes.[4] Copper(I) salts supported by alumina are also involved in the oxychlorination of ethylene.[5] Silver(I) is used industrially for the epoxidation of ethylene to ethylene oxide,[6] and also has found use in numerous alkyne transformations.[7] Likewise, gold catalyzes the hydrochlorination of acetylene to give vinyl chloride,[8] another industrially important chemical, and many processes involving various alkenes and alkynes.[9] Recently, Hashmi reported a bimetallic gold/silver catalyzed alkynylation of cyclopropenes.[9c]

Polydentate ligands comprised of N-containing heterocycles have had a longstanding use in stabilizing isolable coinage metal complexes of small hydrocarbon molecules.[1c] Poly(pyrazolyl)borates are particularly attractive in this regard due to their high degree of steric and electronic tunability through variations of substituents on the pyrazolyl moieties. The tris(pyrazolyl)borate $[HB(3,5\text{-}(CH_3)_2Pz)_3]Cu(C_2H_4)$ (**1**) is the first structurally authenticated copper-ethylene complex.[10] The highly fluorinated tris(pyrazolyl)borate ligand analog $[HB(3,5\text{-}(CF_3)_2Pz)_3]^-$ enabled the isolation of $[HB(3,5\text{-}(CF_3)_2Pz)_3]M(C_2H_4)$ (M = Cu (**2**), Ag (**3**), Au (**4**)), which represents the first complete series of structurally characterized coinage metal (group 11) ethylene complexes.[11] The silver(I) adduct $[HB(3,5\text{-}(CF_3)_2Pz)_3]Ag(C_2H_2)$ is a rare isolable complex featuring a silver-acetylene bond.[11b] $[HB(3,5\text{-}(CF_3)_2Pz)_3]Cu(C_2H_4)$ (**2**) has been utilized in ethylene sensing applications,[12] while the bis(pyrazolyl)borate analog $[H_2B(3,5\text{-}(CF_3)_2Pz)_2]Cu$ is a very effective material for the separation of ethylene from ethane.[13] Furthermore, bis- and tris-(pyrazolyl)borate copper complexes $[H_2B(3,5\text{-}(CF_3)_2Pz)_2]CuNCMe$ and $[HB(3,5\text{-}(CF_3)_2Pz)_3]CuNCMe$ are excellent catalysts for the cyclopropenation of alkynes,[4a] while $[Ph_2B(3\text{-}(CF_3)_2Pz)_2]Cu(C_2H_4)$ mediates alkene cyclopropanation chemistry.[14] The copper complexes such as $[HB(3,5\text{-}(CH_3)_2Pz)_3]Cu(C_2H_4)$ with non-fluorinated tris(pyrazolyl)borate ligand (Figure 1) supports are also proven to be good catalysts for the cyclopropanation of alkenes, cyclopropenation of alkynes, and aziridination of alkenes.[15]

In contrast to the anionic, poly(pyrazolyl)borates (e.g. $[HB(3,5\text{-}(CH_3)_2Pz)_3]^-$, $[H_2B(3,5\text{-}(CH_3)_2Pz)_2]^-$ (**5**)), the closely related neutral poly(pyrazolyl)methanes (e.g., $HC(3,5\text{-}(CH_3)_2Pz)_3$, $H_2C(3,5\text{-}(CH_3)_2Pz)_2$ (**6**)) have been less thoroughly explored.[1c,16] To date, very few bis(pyrazolyl)methane supported olefin complexes have been reported, despite having a similar degree of tunability to their anionic counterparts. For example, in 2006, Pampaloni and coworkers prepared the electron rich bis(pyrazolyl)methane ($H_2C(3,5\text{-}(CH_3)_2Pz)_2$ (**5**)) supported copper(I) complexes of cyclooctene, norbornene, and *p*-vinylanisole.[17] The following year the same group prepared electron poor bis(pyrazolyl)methane ($H_2C(3,5\text{-}(CF_3)_2Pz)_2$) and $H_2C(3\text{-}CF_3Pz)_2$) copper(I) and silver(I) complexes of

[a] *J. Mehara,[+] Prof. Dr. J. Roithová*
Department of Spectroscopy and Catalysis, Institute for Molecules and Materials
Radboud University Nijmegen
Heyendaalseweg 135, 6525 AJ Nijmegen (The Netherlands)
E-mail: J.Roithova@science.ru.nl

[b] *B. T. Watson,[+] A. Noonikara-Poyil, A. O. Zacharias, Prof. H. V. Rasika Dias*
Department of Chemistry and Biochemistry
The University of Texas at Arlington
Arlington, Texas 76019 (USA)
E-mail: dias@uta.edu

[+] *These authors contributed equally.*

Supporting information for this article is available on the WWW under https://doi.org/10.1002/chem.202103984

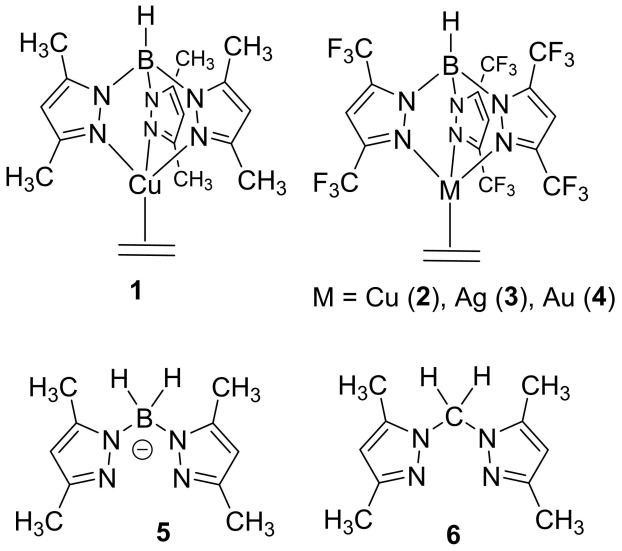

Figure 1. Tris(pyrazolyl)borate coinage metal complexes of ethylene (**1**–**4**), and bis(pyrazolyl) borate (**5**) and bis(pyrazolyl)methane (**6**) supporting ligands.

cyclooctene.[18] However, only $[H_2C(3,5\text{-}(CH_3)_2Pz)_2Cu(cyclooctene)][OTf]$ was characterized using X-ray crystallography. Recently, Sumby and Doonan prepared Mn(II) based MOF using bis[4-carboxyphenyl-(3,5-dimethylpyrazol-1-yl)]methane to trap and characterize copper(I) complexes of CO, ethylene, norbornadiene (NBD) and phenyl acetylene.[19] They also managed to obtained X-ray structural data of the copper ethylene complex, **MnMOF-1**·$[Cu(C_2H_4)][BF_4]$, and the related NBD and phenyl acetylene adducts. Other reported copper and silver complexes of bis(pyrazolyl)methane are typically the homoleptic compounds with two bis(pyrazolyl)methane ligands on metals[16,20] or dimers[17–18,21] which feature bridging bis(pyrazolyl)methane ligands. In addition, there are also quite a few computational studies involving coinage metal complexes of alkenes and alkynes.[22] Overall, isolable and structurally authenticated molecules of copper, silver and gold alkenes and alkynes supported by bis(pyrazolyl)methane ligands are quite rare as evident from the above account.

Furthermore, despite the importance of coinage metals in alkene and alkyne chemistry, there is little experimental evidence on how changing the nature of the ancillary ligand on coinage metal ions and substituents on alkenes and alkynes effect the binding energies of the two components. Previously, we have investigated binding energies of unsaturated hydrocarbons to phosphinogold(I) and phospinosilver(I) ions.[23] The binding energies to alkenes and alkynes were in the range of 1.8–1.9 eV for $[Au(PMe_3)(\pi\text{-ligand})]^+$ and in the range of 1.6–1.8 for $[Au(PPh_3)(\pi\text{-ligand})]^+$.[24] In general, the binding energies were always about 0.1 eV higher for alkynes than for alkenes. In the silver complexes $[Ag(PPh_3)(\pi\text{-ligand})]^+$, the binding energies dropped to the 1.3–1.6 eV range.

In this work, we present results from a systematic study on synthesis, structures, and binding energies involving coinage metal ions and alkenes and alkynes supported by bis(pyrazolyl)methanes. This includes the first X-ray structural data and detailed study of isoleptic, $\{[H_2C(3,5\text{-}(CH_3)_2Pz)_2]M(C_2H_4)\}^+$ series involving the coinage metals, M = Cu, Ag, Au. We also probed the effects of supporting ligand fluorination (and therefore the donor features) on the chemistry of such species. Being a neutral ligand, bis(pyrazolyl)methanes make it an ideal platform for performing mass spectrometric studies to investigate these effects since the complexes of M(I) supported by such ligands are cationic species.

Results

Synthesis and spectroscopic data of alkene and alkyne complexes: The first part of this work involves the isolation of $[LM(\pi\text{-ligand})]^+$ complexes where L represents bidentate, bis(pyrazolyl)methane ligand scaffolds and M was copper, silver, and gold (Figure 2). The properties, spectroscopic, and structural studies of such species were the focus. For this purpose, ethylene complexes $[L_1M(C_2H_4)][SbF_6]$ (M = Cu (**7**), Ag (**8**), Au (**9**)) as well as $[L_3Cu(C_2H_4)][SbF_6]$ (**10**) and $[L_3Ag(C_2H_4)][SbF_6]$ (**11**) were prepared successfully by first generating the tris(ethylene) copper(I), silver(I), or gold(I) hexafluoroantimonate complex in situ,[25] followed by addition of L_1 or L_3 (Scheme 1). The ethylene gas evolution was observed upon addition of the bis(pyrazolyl)methane ancillary ligand. Special care was taken to slowly add a dichloromethane solution of the ancillary ligand during the synthesis of **7**–**11**, to prevent the homoleptic bis-ligand complex ($[(L_x)_2M][SbF_6]$) formation with the loss of bound olefin. Removing solvent under reduced pressure would also result in olefin liberation, also resulting in the aforementioned $[(L_x)_2M][SbF_6]$. Solvent was removed by a slow stream of ethylene to obtain the desired Cu(I), Ag(I), and Au(I) ethylene

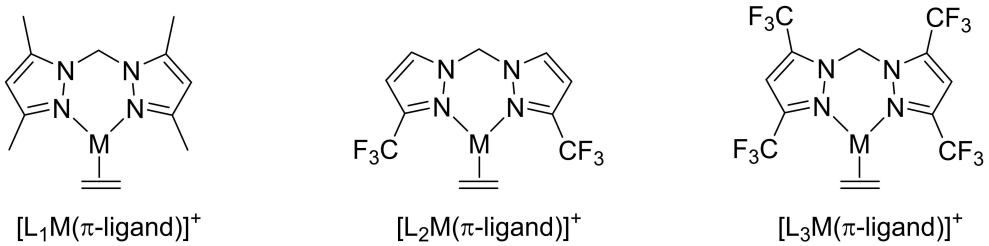

Figure 2. Metal complexes (M = Cu, Ag, Au) with ligands L_1 ($H_2C(3,5\text{-}(CH_3)_2Pz)_2$. **6**), L_2 ($H_2C(3\text{-}(CF_3)Pz)_2$), and L_3 ($H_2C(3,5\text{-}(CF_3)_2Pz)_2$). The π-ligands were various alkenes (ethylene displayed here) and alkynes.

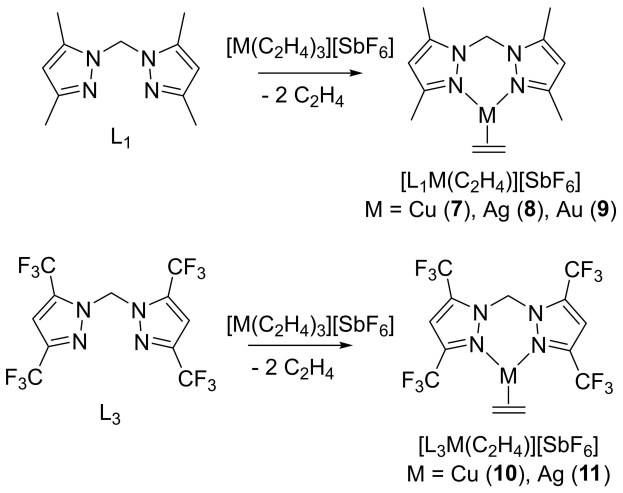

Scheme 1. Synthesis of Cu(I), Ag(I) and Au(I) ethylene complexes supported by ligands L_1 ($H_2C(3,5\text{-}(CH_3)_2Pz)_2$), L_2 ($H_2C(3\text{-}(CF_3)Pz)_2$) and L_3 ($H_2C(3,5\text{-}(CF_3)_2Pz)_2$).

complexes **7**–**11** as colorless crystalline solids. As solids, these compounds are stable under vacuum at room temperature for short periods of time. However, prolonged exposure to reduced pressure will lead to the loss of the coordinated olefins.

The 1-pentene complex $[L_1Cu(1\text{-pentene})][SbF_6]$ (**12**) was also obtained via a similar route[26] using an in situ generated $Cu[SbF_6]$ sample in the presence of excess 1-pentene followed by the addition of L_1 (Scheme 2). The $[L_1Cu(1\text{-pentyne})][SbF_6]$ (**13**) was synthesized by generating the ethylene complex **7** in situ, followed by the addition of excess alkyne (Scheme 2).

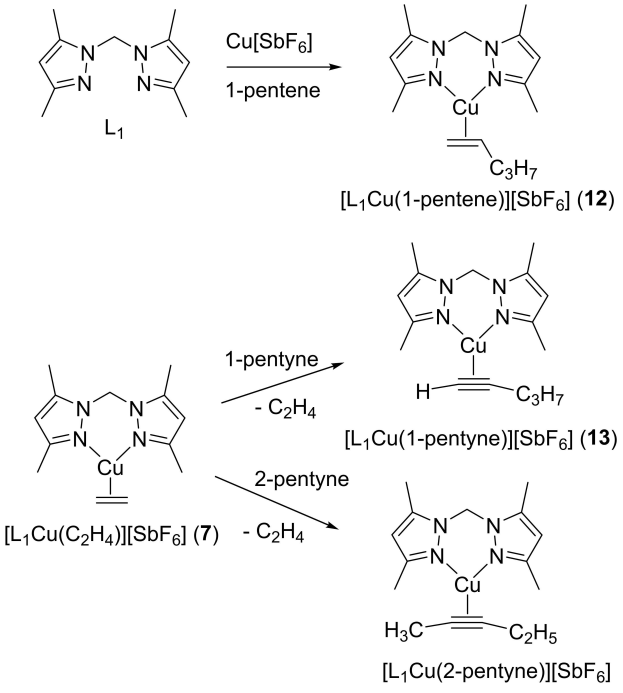

Scheme 2. Synthesis of pentene and pentyne complexes of copper(I) supported by ligands L_1 ($H_2C(3,5\text{-}(CH_3)_2Pz)_2$).

The related 2-pentyne complex of copper(I) was prepared via an analogous method to that of **13**. Attempts to prepare these copper(I) alkyne complexes using the route utilized for **12** and alkynes instead of alkenes were unsuccessful. The solid products of **12** and **13** were obtained by removing the solvent using a nitrogen stream rather than reduced pressure to prevent π-ligand dissociation.

These complexes were characterized by several analytical techniques including ^1H and ^{13}C NMR spectroscopy. The key NMR spectroscopic features of olefinic and alkyne moieties bound to the coinage metal ions are summarized in Table 1. In comparison to the free ethylene, the ^1H and ^{13}C NMR spectra of copper(I) complex **7** show coordination induced upfield shifts of 0.92 ppm and 35.6 ppm for the ethylene protons and carbons, respectively, while the analogous silver(I) complex **8** shows a 0.18 ppm downfield shift of the ethylene proton signals and a 11.6 ppm upfield shift of the carbon resonance (Table 1). The gold(I) complex **9** displayed a noticeably large upfield shift of the ethylene proton and carbon signals (1.70 ppm (^1H) and 66.3 ppm (^{13}C)). The *N,N′*-bis(8-(3,5-dichlorophenyl)-1-naphthyl)butane-2,3-diimine ($Nap'_2Diimine$) ligand supported, cationic coinage metal mono-ethylene adducts, $[(Nap'_2Diimine)M(C_2H_4)][SbF_6]$ reported by Daugulis and co-workers[27] provide a good comparison, and show their ethylene ^{13}C shifts at δ 88.0, 105.4, and 65.4 ppm for M = Cu, Ag and Au, respectively. The group trends are consistent between **7**–**9** and $[(Nap'_2Diimine)M(C_2H_4)][SbF_6]$, as well as with neutral coinage metal ethylene complexes supported by tris(pyrazolyl)borate ligands including the $[PhB(3\text{-}(C_2F_5)Pz)_3]M(C_2H_4)$ series (i.e., the gold and silver complexes displaying the highest and lowest upfield ethylene carbon shifts, respectively, as a result of metal ion coordination).[1c,11, 28] The relative magnitude of the upfield shifts in ethylene carbons due to coordination reflects the σ-acceptor and π-donor abilities of the coinage metal atom (e.g., $d^{10}\rightarrow d^{10}s^1$ electron affinity of Cu(I), Ag(I) and Au(I) ions are −7.72, −7.57 and −9.22 eV, respectively, and $d^{10}\rightarrow d^9p^1$ promotional energies of Cu(I), Ag(I) and Au(I) ions are 8.25, 9.94 and 7.83 eV, respectively),[29] and the extent of M-ethylene π-back bonding believed to exist in these molecules.[28b,30]

Compared to L_1 ($H_2C(3,5\text{-}(CH_3)_2Pz)_2$), the highly fluorinated L_3 ($H_2C(3,5\text{-}(CF_3)_2Pz)_2$) is a weaker donor and should make the metal sites supported by this ligand relatively electron poor. The copper(I) and silver(I) ethylene complexes **10** and **11**, indeed show relatively smaller upfield shifts of the ethylene ^{13}C signal due to metal ion coordination, suggesting somewhat lower level of metal→ethylene backbonding relatively to the related **7** and **8**.[28b,30] The olefinic proton and carbon signals in ^1H and ^{13}C NMR spectra of the 1-pentene complex of copper **12** in acetone-d_6 also shows upfield shifts relative to the corresponding signals of the free 1-pentene, indicating the existence of this adduct in solution. In contrast to the M(olefin) complexes, the 1-pentyne complex **13** displayed large downfield shifts of 2.67 ppm (^1H) and 13.6, 7.6 ppm (^{13}C) in its spectra for the *H*C≡ proton and alkyne carbons. The IR spectrum of **13** displayed bands at 1937 and 3199 cm^{-1}, which can be assigned to the C≡C and ≡C–H stretch. These bands were observed in

Table 1. Selected peaks from ^{1}H and ^{13}C NMR for complexes **7**–**13** and the chemical shift ($\Delta\delta$) from corresponding free π-ligand ($\Delta\delta = \delta$ (metal complex) – δ (free ligand)), $L_1 = H_2C(3,5\text{-}(CH_3)_2Pz)_2$) and $L_3 = H_2C(3,5\text{-}(CF_3)_2Pz)_2$. For comparison, free ethylene has chemical shifts of δ 5.40 (^{1}H) and 123.1 (^{13}C) ppm in $CDCl_3$, 5.40 (^{1}H) and 123.2 (^{13}C) in CD_2Cl_2, and 5.38 (^{1}H) and 123.5 (^{13}C) in acetone-d_6.

compound	^{1}H NMR H_2C=CHR or HC≡CR [ppm]	$\Delta\delta$ [ppm]	^{13}C NMR H_2C=CHR or HC=CR [ppm]	$\Delta\delta$ [ppm]
$[L_1Cu(C_2H_4)][SbF_6]$ (**7**)	4.48[a]	−0.92	87.9[c]	−35.6
$[L_1Ag(C_2H_4)][SbF_6]$ (**8**)	5.56[c]	+0.18	111.9[c]	−11.6
$[L_1Au(C_2H_4)][SbF_6]$ (**9**)	3.70[b]	−1.70	56.9[b]	−66.3
$[L_3Cu(C_2H_4)][SbF_6]$ (**10**)	4.82[c]	−0.56	93.4[c]	−30.1
$[L_3Ag(C_2H_4)][SbF_6]$ (**11**)	5.78[b]	+0.38	113.6[b]	−9.6
$[L_1Cu(1\text{-pentene})][SbF_6]$ (**12**)	4.76, 4.71[c]	−0.21, −0.22	119.4, 94.9[c]	−19.6, −19.5
$[L_1Cu(1\text{-pentyne})][SbF_6]$ (**13**)	4.62[b]	+2.67	98.1, 75.8[b]	+13.6, +7.6

[a] $CDCl_3$, [b] CD_2Cl_2, [c] acetone-d_6

the free 1-pentyne at 2120 and 3307 cm^{-1}, respectively, and thus show red shifts of 183 and 108 cm^{-1}, respectively.

The copper(I)-olefin complexes are moderately air stable, colorless solids, but slowly oxidize to green, presumably copper(II) decomposition products. However, solutions of these olefin complexes are significantly more sensitive to air, and easily produce dark green solutions. The copper(I) complexes of ethylene (**7**, **10**) show poor solubility, except in highly polar solvents such as acetone, tetrahydrofuran, and methanol. Thus, we had to synthesize $[L_1Cu(C_2H_4)]^+$ with a different counter ion $[n\text{-}BuBF_3]^-$ to obtain suitable crystals of $[L_1Cu(C_2H_4)][n\text{-}BuBF_3]$ (**14**) for X-ray crystallographic studies. The gold(I) ethylene complex **9** is somewhat light sensitive and best kept in the dark under an ethylene atmosphere at −20 °C. In solution, we observed partial loss of ethylene from **9** to produce $[L_1Au]^+$ species. It is possible to minimize this ethylene dissociation at lower temperatures. The silver and gold complexes **8** and **9** dissociate and binds ethylene reversibly in solutions when purged with nitrogen gas or ethylene gas as evident from the data from NMR experiments. Remarkably, the 1-pentyne complex **13** was quite shelf stable, even after 6 months of storage.

X-ray crystallographic study: The copper, silver, and gold ethylene complexes, $[L_1Cu(C_2H_4)][n\text{-}BuBF_3]$ (**14**), $[L_1Ag(C_2H_4)][SbF_6]$ (**8**), and $[L_1Au(C_2H_4)][SbF_6]$ (**9**) were isolated using weakly coordinating hexafluoroantimonate and *n*-butyl trifluoroborate anions in order to get a more accurate understanding of the metal-π-ligand interaction between the coinage metal ion and ethylene without significant interference from a coordinating anion. They were characterized by X-ray crystallography and represent a rare, complete series of closely related cationic coinage metal-ethylene complexes with structural data from group trend studies. The coinage metal mono-ethylene adducts, $[(Nap'_2Diimine)Cu(C_2H_4)][OTf]$, $[(Nap'_2Diimine)Ag(C_2H_4)][BF_4]$ and $[(Nap'_2Diimine)Au(C_2H_4)][SbF_6]$ reported by Daugulis and co-workers,[27] and the tris-ethylene complexes $[M(C_2H_4)_3][SbF_6]$[25] and $[M(C_2H_4)_3][Al\{OC(CF_3)_3\}_4]$ (M = Cu, Ag and Au)[31] represent the only other complete series of cationic coinage metal ethylene complexes with X-ray structural data to our knowledge.

Figure 3 depicts the molecular structures of the cationic moieties $[L_1M(C_2H_4)]^+$. They are three-coordinate metal complexes with κ^2-bound $H_2C(3,5\text{-}(CH_3)_2Pz)_2$ ligands. The ethylene coordinates to metal in a familiar η^2-fashion. The cyclic CN_4M core adopts a flattened boat conformation. Table 2 summarizes selected structural parameters. The sum of angles about the metal center in **8**, **9** and **14** is 360°, indicating the trigonal-planer geometry at the metal site. One of the fluorine atoms of $[n\text{-}BuBF_3]^-$ in $[L_1Cu(C_2H_4)][n\text{-}BuBF_3]$ (**14**) sits near Cu at 2.5825(10) Å, which is within the van der Waals contact separation of Cu and F atoms (3.84 Å) but this interaction is not significant to distort the planar geometry at copper. Further-

Table 2. Selected bond lengths and angles of bis(pyrazolyl)methane complexes of Cu, Ag and Au and those of several related complexes for comparisons.

compound	π-ligand C=C [Å]	C–M–C [°]	N–M–N [°]	M–N [Å]	C–M [Å]	Σ angles at M [°] involving N and centroid of C=C
$[L_1Cu(C_2H_4)][n\text{-}BuBF_3]$ (**14**)	1.361(2)	39.44(6)	94.45(4)	1.9885(11), 1.9896(11)	2.0153(13), 2.0181(13)	360
$[L_1Ag(C_2H_4)][SbF_6]$ (**8**)	1.350(5)	34.96(12)	88.96(9)	2.223(2), 2.232(2)	2.243(3), 2.253(3)	360
$[L_1Au(C_2H_4)][SbF_6]$ (**9**)	1.401(3)	39.04(10)	87.37(7)	2.1720(19), 2.1733(18)	2.098(2), 2.094(2)	360
$[PhB(3\text{-}(C_2F_5)Pz)_3]Cu(C_2H_4)$[28a]	1.354(7)	38.96(19)	93.76(13)	2.008(3), 2.009(3)	2.027(4), 2.033(4)	360
$[PhB(3\text{-}(C_2F_5)Pz)_3]Ag(C_2H_4)$[28a]	1.311(5)	33.38(14)	86.02(7)	2.279(2), 2.286(2)	2.286(3), 2.279(3)	360
$[PhB(3\text{-}(C_2F_5)Pz)_3]Au(C_2H_4)$[28a]	1.366(12)	38.0(3)	84.7(2)	2.213(6), 2.216(6)	2.089(8), 2.105(7)	360
$[L_3Ag(C_2H_4)][SbF_6]$ (**11**)[a]	1.340(4); 1.340(4)	33.67(11); 33.69(11)	86.44(6); 86.49(6)	2.3306(18), 2.3328(18); 2.3330(18), 2.3293(18)	2.309(3), 2.319(3); 2.312(3), 2.313(3)	359.7; 359.8
$[L_1Cu(1\text{-pentene})][SbF_6]$ (**12**)	1.364(3)	39.14(8)	95.69(6)	1.9816(14), 1.9936(14)	2.0194(18), 2.0512(17)	359.0
$[L_1Cu(coe)][OTf]$[17] (**15**)	1.362(3)	38.57(9)	94.57(9)	2.007(2), 2.009(2)	2.072(2), 2.050(2)	354.2[b]
$[L_1Cu(1\text{-pentyne})][SbF_6]$ (**13**)	1.241(2)[c]	36.64(6)	91.93(5)	1.9787(11), 1.9856(12)	1.9540(14), 1.9927(14)	359.8[d]

[a] two molecules in the asymmetric unit, [b] triflate counterion excluded in the calculation of sum of angles, [c] C≡C length, [d] involving centroid of C≡C

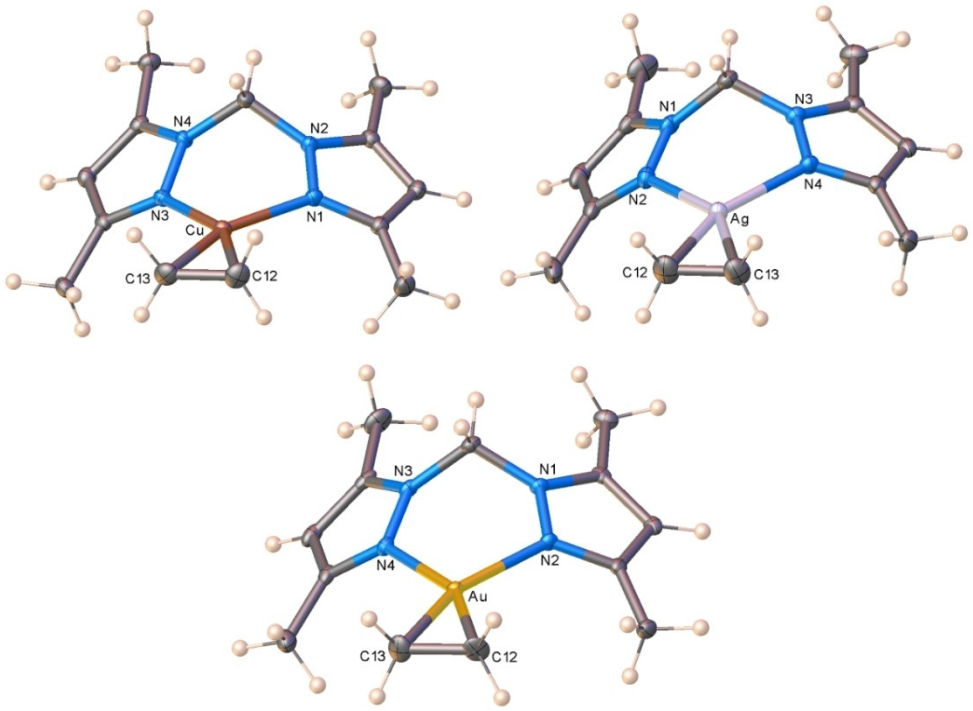

Figure 3. Molecular structures of $[L_1Cu(C_2H_4)][n\text{-}BuBF_3]$ (**14**), $[L_1Ag(C_2H_4)][SbF_6]$ (**8**), and $[L_1Au(C_2H_4)][SbF_6]$ (**9**) (clockwise from top to bottom). Anions have been omitted for clarity. $L_1 = H_2C(3,5\text{-}(CH_3)_2Pz)_2$ (**6**)

more, Cu(I) complexes of terminal fluoride ligands usually have much shorter Cu–F distances, for example, [(*t*-Bu)$_2$phen]CuF (1.870(8) Å),[32] $(PPh_3)_3CuF$ (2.062(6) Å).[33]

The N–M–N and C–M–C planes are nearly coplanar with torsion angles of 1.85°, 5.67°, and 2.12° for $[L_1M(C_2H_4)]^+$ (M = Cu, Ag and Au, respectively), with the silver adduct showing the largest twist perhaps suggesting the weakest M-ethylene π-back bonding. The Cu–N < Au–N < Ag–N bond length follows the covalent radii, as silver is bigger than both gold and copper.[34] The M–C bond lengths also follow this trend, and they compare well with the previously reported tris(pyrazolyl)borate ligand supported coinage metal ethylene complexes[1c,11c, 28] and copper and silver dipyridyl amine systems involving larger olefins.[35] The ethylene C=C bond is longest for $[L_1Au(C_2H_4)]^+$, followed by $[L_1Cu(C_2H_4)]^+$ and $[L_1Ag(C_2H_4)]^+$ with bond lengths of 1.401(3), 1.361(2), and 1.350(5) Å, respectively, but the difference in the latter two numbers is not significant at the 3σ limit of estimated standard deviations (for comparison, the C=C bond length for free gaseous ethylene is 1.3305(10) Å while the corresponding distance from X-ray data is 1.313 Å).[36] Apart from the MOF complex **MnMOF-1**·$[Cu(C_2H_4)]BF_4$,[19] there are no structurally characterized bis(pyrazolyl)methane adducts of Cu, Ag or Au with ethylene to our knowledge. The M–N, M–C, and C=C bond lengths of $[L_1M(C_2H_4)]^+$ are however, consistent with the structural data on molecules supported by various other supporting ligands, which suggests that gold interacts strongest with ethylene, followed by copper while silver having the weakest interaction with ethylene.[27–28,37]

We have also managed to crystallize and characterize $[L_3Ag(C_2H_4)][SbF_6]$ (**11**) that has a highly fluorinated bis(pyrazolyl)methane supporting ligand, $H_2C(3,5\text{-}(CF_3)_2Pz)_2$ using single crystal X-ray crystallography (Figure 4). Basic structural features are similar between $[L_1Ag(C_2H_4)][SbF_6]$ and $[L_3Ag(C_2H_4)][SbF_6]$. The $[L_3Ag(C_2H_4)][SbF_6]$ is also a three-coordinate, trigonal planar metal complex. The Ag–N and Ag–C distances are significantly longer in the $[L_3Ag(C_2H_4)][SbF_6]$ compared to those of the $[L_1Ag(C_2H_4)][SbF_6]$ pointing to the relatively weakly coordinating nature of $H_2C(3,5\text{-}(CF_3)_2Pz)_2$ in comparison to $H_2C(3,5\text{-}(CH_3)_2Pz)_2$ (Table 2). This observation is in agreement with the NMR data presented above for the two adducts (i.e., $[L_1Ag(C_2H_4)][SbF_6]$ and $[L_3Ag(C_2H_4)][SbF_6]$ display chemical shifts

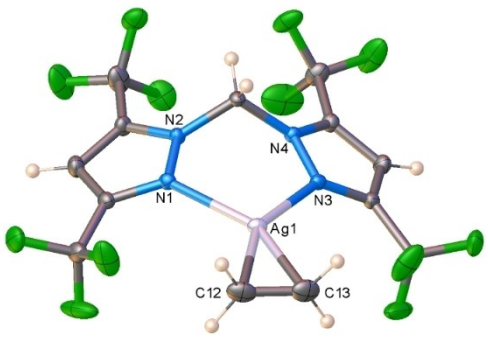

Figure 4. Molecular structure of $[L_3Ag(C_2H_4)][SbF_6]$ (**11**). The anion has been omitted for clarity. $L_3 = H_2C(3,5\text{-}(CF_3)_2Pz)_2$

of 5.56 and 5.78 ppm in their ^{1}H spectra and 111.9 and 113.6 ppm in their ^{13}C spectra for the ethylene moiety). However, the C=C distance is not significantly different between the two complexes, which is not unusual,[28b,38] considering typically smaller changes in the distances are often overshadowed by the relatively high estimated standard deviations (esds) associated with the measurement, libration effects and anisotropy of the electron density.

We have also investigated the 1-pentene and 1-pentyne complexes, [L_1Cu(1-pentene)][SbF_6] (**12**) and [L_1Cu(1-pentyne)][SbF_6] (**13**) using X-ray crystallography. The molecular structures are illustrated in Figure 5. They are three-coordinate metal complexes with κ^2-bound $H_2C(3,5\text{-}(CH_3)_2Pz)_2$ ligands. Pentene and pentyne coordinate to copper in the typical η^2-fashion. The cyclic CN_4Cu core in these molecules adopts a flattened boat conformation. The N–M-N and C–M–C planes are not strictly coplanar with torsion angles of 9.63° and 5.20° for [L_1Cu(1-pentene)][SbF_6] and [L_1Cu(1-pentyne)][SbF_6], respectively.

The C=C bond length of 1.364(3) Å of [L_1Cu(1-pentene)][SbF_6] is similar to the corresponding distance observed in the ethylene complex **14** (1.361(2) Å). The bending back angle between the CuC_1C_2 plane and the $C_1C_2C_3$ plane of 1-pentene is 9.9° deviated from the idealized 90°, illustrating the effect of σ/π-interaction between the copper(I) to 1-pentene in **12**. A copper(I)-cyclooctene complex, [L_1Cu(coe)][OTf][17] (**15**) supported by L_1 is known, but this molecule features a short TfO–Cu contact leading to a pseudo-tetrahedral copper site (Table 2). The Cu–C and Cu–N distances of **15** are slightly longer than the corresponding distances observed for **12**.

The C≡C bond length of [L_1Cu(1-pentyne)][SbF_6] (1.241(2) Å) is at the upper end of the few reported three-coordinate, terminal copper(I) alkynes of the type N_2Cu(alkyne) in the literature.[39] The C≡C–C bond angle of 160.85(14)° is typical[2c] and shows a significant deviation from linearity as a result of the copper-coordination. For comparison, the neutral copper(I)-hexyne complex, [N{(C_3F_7)C(Dipp)N}$_2$]Cu(EtC≡CEt) has C≡C–C bond angles of 156.5(2)° and 156.3(2)°.[40] Packing diagrams of **8, 9, 11–14** show contacts between some fluorine atoms of the anion and some hydrogen atoms of the cationic moieties, as well as between the Cu site and one of the fluorines in compound **14**.

Mass spectroscopic studies: Next, we investigated bond dissociation energies in mass-selected cationic [LM(π-ligand)]$^+$ complexes with L = L_1, L_2, and L_3 (Tables 3 and 5 and Figure 6). Despite all efforts, it was impossible to generate gaseous complexes with ethylene or acetylene. However, we could prepare a series of [L_1M(π-ligand)]$^+$ complexes with larger terminal and internal alkenes and alkynes. We were not able to generate all complexes with the more electron-deficient ligands L_2 and L_3, therefore we will discuss the general trends for the complexes with the L_1 ligand first.

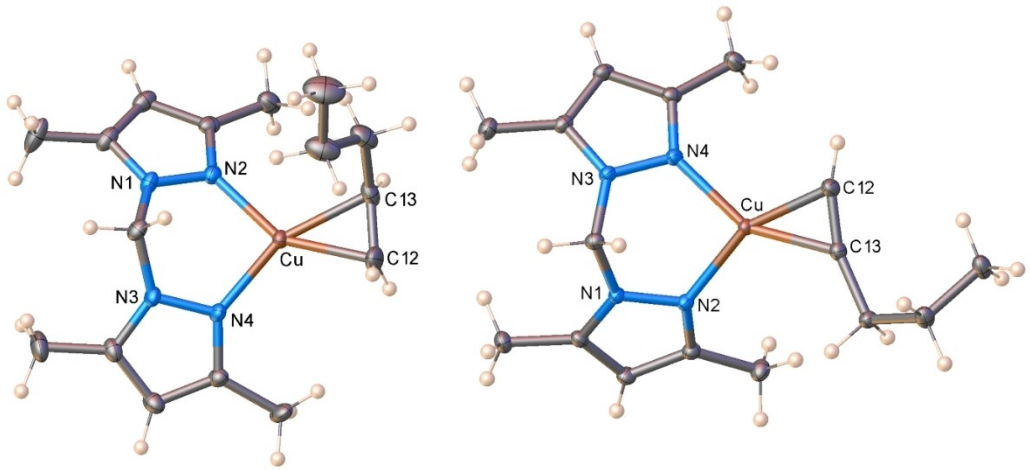

Figure 5. Molecular structures of [L_1Cu(1-pentene)][SbF_6] (**12**, left) and [L_1Cu(1-pentyne)][SbF_6] (**13**, right). The anions were omitted for clarity. $L_1 = H_2C(3,5\text{-}(CH_3)_2Pz)_2$

Table 3. Bond dissociation energies of π-ligands from [L_1M(π-ligand)]$^+$. $L_1 = H_2C(3,5\text{-}(CH_3)_2Pz)_2$.

π-Ligand	[L_1Cu(π-ligand)]$^+$		[L_1Ag(π-ligand)]$^+$		[L_1Au(π-ligand)]$^+$	
	BDE_{exp} [eV]	BDE_{theor} [eV]	BDE_{exp} [eV]	BDE_{theor} [eV]	BDE_{exp} [eV]	BDE_{theor} [eV]
1-Pentene	1.51 ± 0.02	1.40	1.21 ± 0.01	1.16	1.94 ± 0.01	1.95
2-Pentene	1.46 ± 0.01	1.33	1.20 ± 0.04	1.12	1.95 ± 0.04	1.90
1-Pentyne	1.63 ± 0.02	1.48	1.21 ± 0.03	1.16	1.92 ± 0.04	1.96
2-Pentyne	1.65 ± 0.02	1.52	1.30 ± 0.02	1.21	2.09 ± 0.04	2.02
3-Hexyne	1.73 ± 0.03	1.58	1.36 ± 0.01	1.27	2.11 ± 0.04	2.09
Styrene	1.54 ± 0.01	1.51	1.24 ± 0.04	1.21	1.95 ± 0.01	1.97
Phenylacetylene	1.67 ± 0.01	1.54	1.23 ± 0.01	1.22	1.97 ± 0.01	1.99
1-Phenylpropyne	1.66 ± 0.02	1.57	1.31 ± 0.02	1.27	2.09 ± 0.01	2.05

Table 4. Bond dissociation energies of π-ligands from $[L_2M(\pi\text{-ligand})]^+$. $L_2 = H_2C(3\text{-}(CF_3)Pz)_2$.

π-Ligand	$[L_2Cu(\pi\text{-ligand})]^+$		$[L_2Ag(\pi\text{-ligand})]^+$		$[L_2Au(\pi\text{-ligand})]^+$	
	BDE_{exp} [eV]	BDE_{theor} [eV]	BDE_{exp} [eV]	BDE_{theor} [eV]	BDE_{exp} [eV]	BDE_{theor} [eV]
1-Pentene		1.60	1.31 ± 0.03	1.31	1.92 ± 0.01	2.20
2-Pentene		1.54	1.29 ± 0.07	1.29	1.95 ± 0.01	2.17
1-Pentyne	1.62 ± 0.01	1.67	1.35 ± 0.02	1.32	1.75 ± 0.08	2.19
2-Pentyne	1.64 ± 0.01	1.69	1.41 ± 0.02	1.39	1.97 ± 0.03	2.27

Table 5. Bond dissociation energies of π-ligands from $[L_3M(\pi\text{-ligand})]^+$. $L_3 = H_2C(3,5\text{-}(CF_3)_2Pz)_2$.

π-Ligand	$[L_3Cu(\pi\text{-ligand})]^+$		$[L_3Ag(\pi\text{-ligand})]^+$		$[L_3Au(\pi\text{-ligand})]^+$	
	BDE_{exp} [eV]	BDE_{theor} [eV]	BDE_{exp} [eV]	BDE_{theor} [eV]	BDE_{exp} [eV]	BDE_{theor} [eV]
1-Pentene	1.50	1.65	1.26 ± 0.02	1.36		2.24
2-Pentene	1.47	1.60	1.28 ± 0.04	1.35		2.24
1-Pentyne	1.60 ± 0.02	1.71	1.30 ± 0.01	1.37		2.19
2-Pentyne	1.62 ± 0.03	1.74	1.34 ± 0.04	1.43		2.30

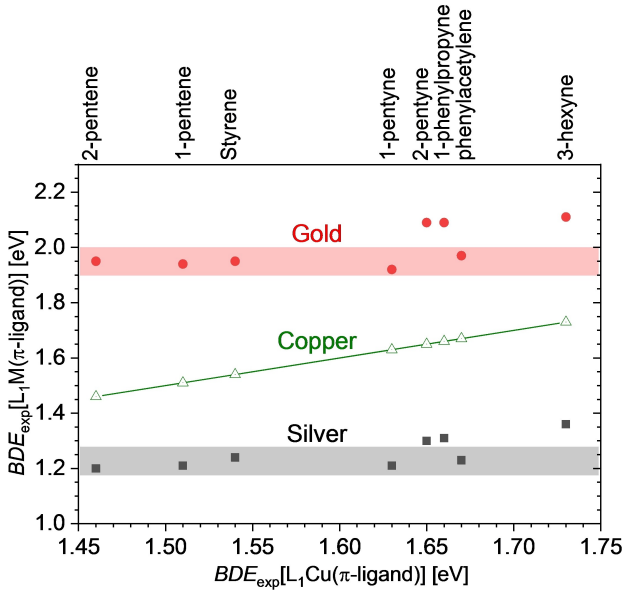

Figure 6. The relation between the experimental *BDE*s of π-ligands in $[L_1Ag(\pi\text{-ligand})]^+$ and $[L_1Au(\pi\text{-ligand})]^+$ and those in $[L_1Cu(\pi\text{-ligand})]^+$ (Table 3). $L_1 = H_2C(3,5\text{-}(CH_3)_2Pz)_2$

In the series of the metal complexes, the binding energies to the π ligands increase going from the silver to the copper and finally to the gold complexes (Table 3). This observation is consistent with the data from spectroscopic and structural studies described above. The copper complex binds with a larger energy to the alkynes than to the alkenes (see distribution along x-axis in Figure 6). Silver and gold complexes bind with a similar binding energy to alkenes and terminal alkynes (~1.2 eV in $[L_1Ag(\pi\text{-ligand})]^+$ and ~1.9 eV in $[L_1Au(\pi\text{-ligand})]^+$, see the color-highlighted stripes in Figure 6). The internal alkynes have about 0.1–0.2 eV larger binding energies in both, silver, and gold complexes (see the point above the color-highlighted stripes in Figure 6). For all the investigated complexes, the symmetrical 3-hexyne has the largest binding energy. Interestingly, Widenhoefer has also observed such unusual binding involving 3-hexyne with phosphine supported gold (I).[41] An easily isolable, isoleptic series $[N\{(C_3F_7)C\text{-}(Dipp)N\}_2]M(EtC{\equiv}CEt)$ (M = Cu, Ag and Au) is also known with 3-hexyne.[40]

We have further calculated the bond dissociation energies of the π-ligands in the $[L_1M(\pi\text{-ligand})]^+$ complexes using DFT theory (B3LYP-D3/def2TZVPP). In a rough approximation, the experimental data correlate well with the theory (see the solid points in Figure 7 and their grouping around the dashed correlation lines). We find the best agreement between the theoretical and experimental values of the gold complexes. In the case of the silver and copper complexes, the values correlate well, but the theoretical bonding energies are underestimated by about 0.05 eV for the silver complexes and by about 0.1 eV for the copper complexes. However, in a more detailed inspection of individual metal complexes series, the trend of the *BDE*s of different π-ligands correlates well only for the copper complexes except for the *BDE*s for styrene and 1-phenylpropyne (see Figure S36). The prediction of the *BDE* trend in the silver (Figure S37) and gold complexes (Figure S38) is less precise.

Next, we have compared the binding energies in complexes with modified ligands L_1–L_3 (Figure 7, Tables 3–5). The electron deficient ligands could be expected to promote a stronger σ-bonding associated with the electron density transfer from the π-ligands to the metal centers but should have a weaker π-back bonding interaction. The experiments show that the *BDE*s of the given π-ligands slightly decreased when the ancillary ligand was more electron deficient (see the y-values of the connected points in Figure 7; for details see Figures S39–S41) pointing to the importance of the π-back bonding. That trend is in agreement with the reported DFT data on three-coordinate, gold tris(pyrazolyl)borate complexes.[42] Note that the formation of the complexes with the electron deficient ligands L_2 and L_3 was difficult and therefore we couldn't measure whole series of the complexes. The gold complexes with L_3 were not formed at all.

In order to confirm the trend of the binding energies, we have also measured IR photodissociation spectra of selected gaseous complexes. The focus was on complexes with 1-

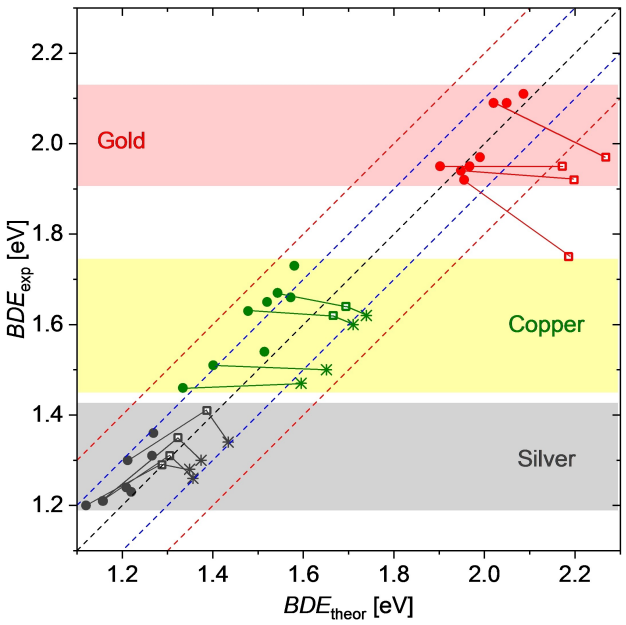

Figure 7. The relation between theoretically calculated *BDE*s of π-ligands in copper, silver, and gold complexes (green, black, and red, respectively) $[L_1M(\pi\text{-ligand})]^+$ (solid circles), $[L_2M(\pi\text{-ligand})]^+$ (open squares), $[L_3M(\pi\text{-ligand})]^+$ (stars) (listed in Tables 3–5). The color-coded lines connect points corresponding to the complexes with the same π-ligand, but different L. $L_1 = H_2C(3,5\text{-}(CH_3)_2Pz)_2$, $L_2 = H_2C(3\text{-}(CF_3)Pz)_2$ and $L_3 = H_2C(3,5\text{-}(CF_3)_2Pz)_2$

pentyne as they show a prominent C≡C stretching vibration. The spectral shifts of this vibration can also be related to the effect of the metal binding on the C≡C bond. The ν_{CC} of free 1-pentyne is 2120 cm^{-1}.[43] We have first compared the C≡C stretching vibrations in copper, silver, and gold complexes with the L_1 ligand (Figure 8). In agreement with the predicted trend of binding energies, we observed the smallest red shift for the silver complex (ν_{CC} = 2024 cm^{-1}), followed by the copper complex (ν_{CC} = 1947 cm^{-1}) and by the gold complex with the largest red shift (ν_{CC} = 1862 cm^{-1}). The stretching frequency of the $L_1Cu(1\text{-pentyne})^+$ agreed well with the isolated solid complex (ν_{CC} = 1937 cm^{-1} in both the Raman and infrared). The remaining part of the fingerprint spectra nicely correspond to the theoretically predicted bands (see Figures S42–S44).

Next, we investigated series of copper complexes with 1-pentyne and the ligands L_1, L_2, and L_3 (Figure 9). The IR photodissociation spectra clearly show that the red shift of the C≡C stretching vibration is slightly smaller for the complexes with electron deficient ligands (L_1: 1947 cm^{-1}, L_2: 1977 cm^{-1}, L_3: 1980 cm^{-1}). Similarly, we could compare the IR spectra of silver complexes with L_1 and L_3 and the trend (L_1: 2024 cm^{-1}, L_3: 2035 cm^{-1}) again clearly showed a weaker interaction of the alkyne with the complex bearing the electron deficient ligand L_3. These spectroscopic data thus fully support the experimental binding energies and show that the more electron deficient ancillary ligands do not support a stronger interaction between the coinage metals and the π-ligands.

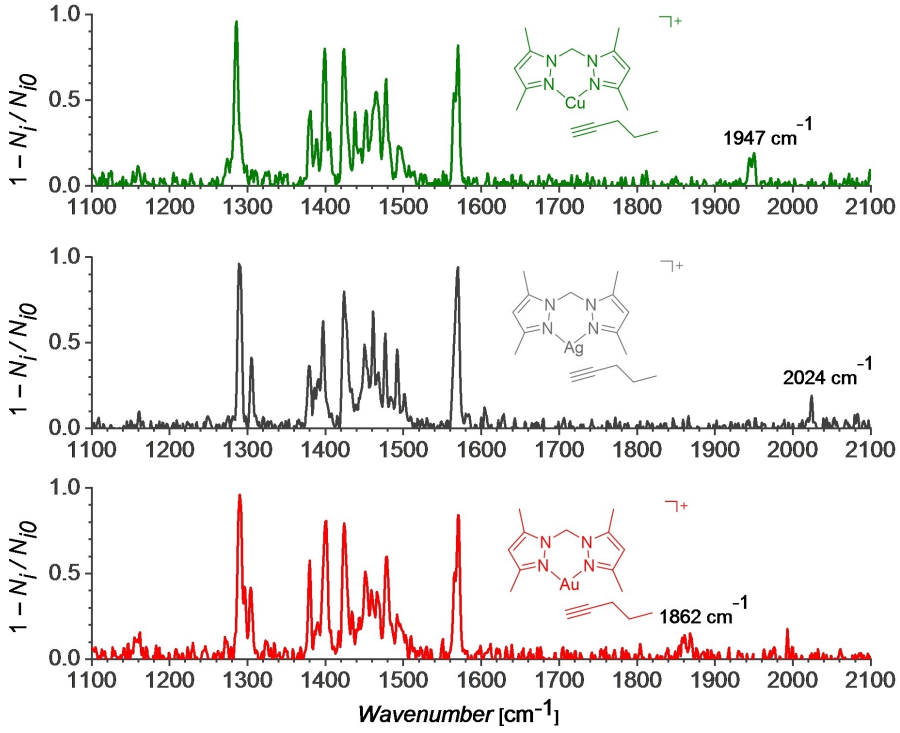

Figure 8. Helium tagging photodissociation spectra of $[L_1Cu(1\text{-pentyne})]^+$(top, green), $[L_1Ag(1\text{-pentyne})]^+$ (middle, grey), and$[L_1Au(1\text{-pentyne})]^+$ (bottom, red). The fingerprint IR spectrum agrees with the theoretically predicted spectra (Figures S42–S44). $L_1 = H_2C(3,5\text{-}(CH_3)_2Pz)_2$

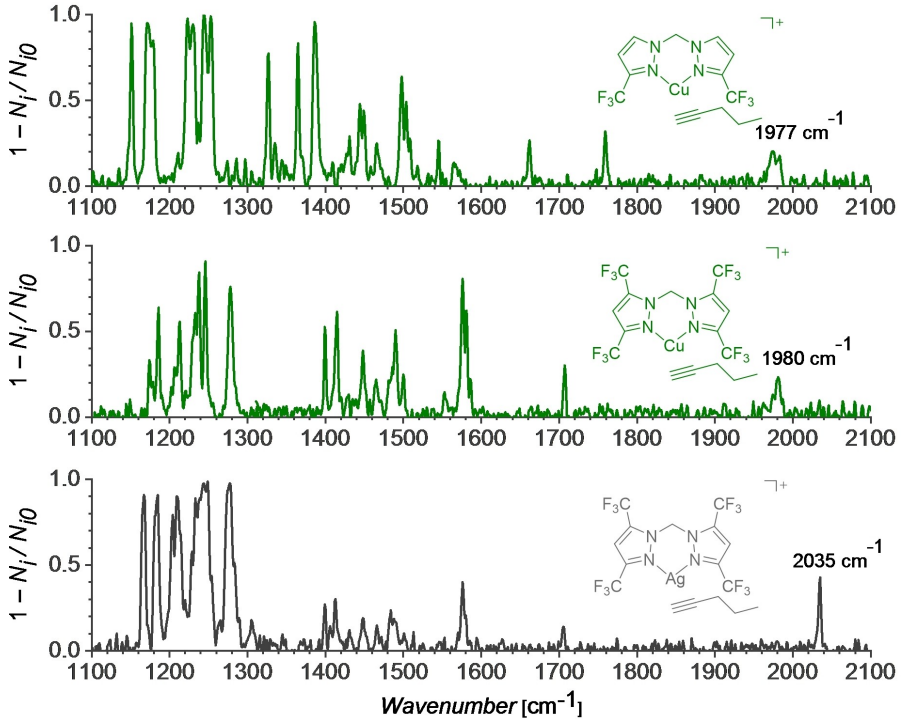

Figure 9. Helium tagging photodissociation spectra of $[L_2Cu(1\text{-pentyne})]^+$ and $[L_3Cu(1\text{-pentyne})]^+$ (top and middle, both green) and $[L_3Ag(1\text{-pentyne})]^+$ (bottom, grey). The fingerprint IR spectrum agrees well with the theoretically predicted spectra (Figures S45–S47). $L_2 = H_2C(3\text{-}(CF_3)Pz)_2$ and $L_3 = H_2C(3,5\text{-}(CF_3)_2Pz)_2$

Discussion

We have reported a series of π-complexes with copper(I), silver(I), and gold(I) having bidentate ancillary ligands. The binding energies of the π-ligands increase in the complexes in the order of Ag < Cu < Au (Table 3). This trend correlates with the increasing C–C bond distances of the π-bonds of the ligands in the corresponding crystal structures (Table 2). In solution, the increasing binding energy correlates with the increasing up-field NMR shifts of the carbon atoms of the coordinated multiple bond as well as with the up-field NMR shifts of the hydrogen atoms attached to those carbon atoms (Table 1). The effect on the NMR shifts is almost negligible for the silver complexes but increases for the copper- and even more for the gold complexes. These results suggest that the binding between the coinage metals Cu^I and Au^I and the π-ligands leads to an increase of electron density at the π-bond and thus is dominantly mediated by π-back bonding in these complexes. This finding is in agreement with recent computational analysis of three-coordinate coinage metal complexes bearing nitrogen-based supporting ligands.[14,42, 44] Interestingly, the computational data of the coinage metal ethylene and acetylene complexes without supporting ligands predict the presence of more dominant σ-bonding interaction over π-back bonding.[45]

The importance of the π-back bonding for the interactions in the reported complexes is further highlighted by a neutral- or a negative effect of electron-withdrawing substituents at the ancillary ligands on the binding energies between the metals and π-ligands. The electron-withdrawing substitution at the ancillary ligands decreases electron density at the metals. Therefore, it should support σ-bonding interaction between the π-ligands and the metals but should weaken the π-back bonding. The experimental data show that upon the reducing of the electron density at the metal, the binding energies slightly grow for silver complexes, stay about the same for copper complexes and decrease for the gold complexes. The trend suggests that the role of the π-back bonding grows in the series Ag < Cu < Au and is probably the dominating interaction for the gold π-complexes.[42]

Finally, a comparison of the experimental *BDE* data with non-relativistic DFT calculations presented above (Figure 7) shows that DFT does not correctly describe the effects of electron-withdrawing substituents at the ancillary ligands on metal-π-ligand moiety. This is probably due to an insufficient description of the π-back bonding at the nonrelativistic level.[46a] Accordingly, the agreement for the gold complexes is the worst. The relativistic effects destabilize the 5d electrons that are therefore high in energy and thus can more efficiently participate in the binding interactions with π ligands.[46b] If this relativistic effect is insufficiently included in the calculations, the participation of the d-electrons in the binding will be underestimated leading to a wrong description of the π-back bonding.

Conclusions

The bis(pyrazolyl)methane ligands enabled a detailed investigation of coinage metal alkene and alkyne complexes including the solid state structural data on a rare isoleptic series $[L_1M(C_2H_4)]^+$ (M = Cu, Ag, Au). The interaction between these transition metals and π-ligands is a combination of σ bonding and π-back bonding. Consistent with NMR spectroscopic and X-ray structural data, and in agreement with previous studies, this shows that the binding energies of π-ligands in the coinage metal complexes increase in the series Ag < Cu < Au.[47] It is often believed that the σ bonding contribution for the d^{10} coinage metal complexes prevails over the π-back bonding contribution. However, the experimental trend of binding energies and geometry parameters does not support this hypothesis. On contrary, the π-ligand binding energies for copper and gold complexes decrease with the electron withdrawing substitution on the ancillary ligands. This suggest that the π-back bonding interaction play a significant role in this type of complexes, even though they are cationic, closed-shell d^{10} metal systems.

Supporting Information Available: Experimental details, synthesis, X-ray crystallographic data (CIF, CCDC deposition numbers 2113041–2113046), NMR and IR/Raman spectroscopic data of metal complexes, additional data obtained by MS experiments, helium tagging photodissociation spectroscopy, and DFT calculations.

Deposition Numbers 2113041 (for **14**), 2113042 (for **8**), 2113043 (for **9**), 2113044 (for **11**), 2113045 (for **12**) and 2113045 (for **13**) contain the supplementary crystallographic data for this paper. These data are provided free of charge by the joint Cambridge Crystallographic Data Centre and Fachinformationszentrum Karlsruhe Access Structures service.

Acknowledgements

This material is based upon work supported by the National Science Foundation under grant number (CHE-1954456, HVRD), Robert A. Welch Foundation (Grant Y-1289, HVRD) and European Research Council (ERC CoG No. 682275).

Conflict of Interest

The authors declare no conflict of interest.

Data Availability Statement

The data that support the findings of this study are available from the corresponding author upon reasonable request.

Keywords: alkene ligands · alkyne ligands · bond energy · mass spectrometry · X-ray diffraction

[1] a) A. M. Echavarren, N. Jiao, V. Gevorgyan, *Chem. Soc. Rev.* **2016**, *45*, 4445–4447; b) M. M. Diaz-Requejo, P. J. Perez, *Chem. Rev.* **2008**, *108*, 3379–3394; c) H. V. R. Dias, C. J. Lovely, *Chem. Rev.* **2008**, *108*, 3223–3238; d) A. J. Jordan, G. Lalic, J. P. Sadighi, *Chem. Rev.* **2016**, *116*, 8318–8372; e) A. S. K. Hashmi, *Chem. Rev.* **2021**, *121*, 8309–8310; f) G. Dyker, *Angew. Chem. Int. Ed.* **2000**, *39*, 4237.

[2] a) J. E. Hein, V. V. Fokin, *Chem. Soc. Rev.* **2010**, *39*, 1302–1315; b) E. Haldón, M. C. Nicasio, P. J. Pérez, *Org. Biomol. Chem.* **2015**, *13*, 9528–9550; c) D. Parasar, T. T. Ponduru, A. Noonikara-Poyil, N. B. Jayaratna, H. V. R. Dias, *Dalton Trans.* **2019**, *48*, 15782–15794.

[3] a) B. Angulo, C. I. Herrerías, Z. Hormigón, J. A. Mayoral, L. Salvatella, *J. Mol. Model.* **2018**, *24*, 195; b) M. P. A. Lyle, N. D. Draper, P. D. Wilson, *Org. Biomol. Chem.* **2006**, *4*, 877–885; c) S. T. Handy, A. Ivanow, *Inorg. Chim. Acta* **2009**, *362*, 4468–4471; d) C. Martín, J. M. Muñoz-Molina, A. Locati, E. Alvarez, F. Maseras, T. R. Belderrain, P. J. Pérez, *Organometallics* **2010**, *29*, 3481–3489.

[4] a) A. Noonikara-Poyil, S. G. Ridlen, H. V. R. Dias, *Inorg. Chem.* **2020**, *59*, 17860–17865; b) M. M. Díaz-Requejo, M. A. Mairena, T. R. Belderrain, M. C. Nicasio, S. Trofimenko, P. J. Pérez, *Chem. Commun.* **2001**, 1804–1805; c) P. Rodríguez, A. Caballero, M. M. Díaz-Requejo, M. C. Nicasio, P. J. Pérez, *Org. Lett.* **2006**, *8*, 557–560; d) J. Pérez, D. Morales, L. A. García-Escudero, H. Martínez-García, D. Miguel, P. Bernad, *Dalton Trans.* **2009**, 375–382; e) H. Martínez-García, D. Morales, J. Pérez, M. Puerto, D. Miguel, *Inorg. Chem.* **2010**, *49*, 6974–6985; f) C. Martín, M. Sierra, E. Alvarez, T. R. Belderrain, P. J. Pérez, *Dalton Trans.* **2012**, *41*, 5319–5325; g) L. Maestre, E. Ozkal, C. Ayats, Á. Beltrán, M. M. Díaz-Requejo, P. J. Pérez, M. A. Pericàs, *Chem. Sci.* **2015**, *6*, 1510–1515.

[5] C. Lamberti, C. Prestipino, L. Capello, S. Bordiga, A. Zecchina, G. Spoto, S. D. Moreno, A. Marsella, B. Cremaschi, M. Garilli, S. Vidotto, G. Leofanti, *Int. J. Mol. Sci.* **2001**, *2*.

[6] a) J. K. Plischke, A. J. Benesi, M. Albert Vannice, *J. Catal.* **1992**, *138*, 223–239; b) H. V. R. Dias, Z. Wang, *Inorg. Chem.* **2000**, *39*, 3724–3727; c) S. Böcklein, S. Günther, R. Reichelt, R. Wyrwich, M. Joas, C. Hettstedt, M. Ehrensperger, J. Sicklinger, J. Wintterlin, *J. Catal.* **2013**, *299*, 129–136; d) J. Roithová, D. Schröder, *J. Am. Chem. Soc.* **2007**, *129*, 15311–15318.

[7] G. Fang, X. Bi, *Chem. Soc. Rev.* **2015**, *44*, 8124–8173.

[8] a) Y. Li, C. Zhang, H. Zhang, L. Li, J. Zhang, R. Oh, L. Yao, M. Cai, J. Li, M. Zhang, F. Li, *App. Catal. A: General* **2021**, *612*, 118015; b) Z. Chen, Y. Chen, S. Chao, X. Dong, W. Chen, J. Luo, C. Liu, D. Wang, C. Chen, W. Li, J. Li, Y. Li, *ACS Catal.* **2020**, *10*, 1865–1870.

[9] a) A. S. K. Hashmi, *Chem. Rev.* **2007**, *107*, 3180–3211; b) Z. Li, C. Brouwer, C. He, *Chem. Rev.* **2008**, *108*, 3239–3265; c) Y. Yang, P. Antoni, M. Zimmer, K. Sekine, F. F. Mulks, L. Hu, L. Zhang, M. Rudolph, F. Rominger, A. S. K. Hashmi, *Angew. Chem. Int. Ed.* **2019**, *58*, 5129–5133; *Angew. Chem.* **2019**, *131*, 5183–5187.

[10] J. S. Thompson, R. L. Harlow, J. F. Whitney, *J. Am. Chem. Soc.* **1983**, *105*, 3522–3527.

[11] a) H. V. R. Dias, H.-L. Lu, H.-J. Kim, S. A. Polach, T. K. H. H. Goh, R. G. Browning, C. J. Lovely, *Organometallics* **2002**, *21*, 1466–1473; b) H. V. R. Dias, Z. Wang, W. Jin, *Inorg. Chem.* **1997**, *36*, 6205–6215; c) H. V. R. Dias, J. Wu, *Angew. Chem. Int. Ed.* **2007**, *46*, 7814–7816; *Angew. Chem.* **2007**, *119*, 7960–7962.

[12] a) B. Esser, T. M. Swager, *Angew. Chem. Int. Ed.* **2010**, *49*, 8872–8875; *Angew. Chem.* **2010**, *122*, 9056–9059; b) B. Esser, J. M. Schnorr, T. M. Swager, *Angew. Chem. Int. Ed.* **2012**, *51*, 5752–5756; *Angew. Chem.* **2012**, *124*, 5851–5855.

[13] A. Noonikara-Poyil, H. Cui, A. A. Yakovenko, P. W. Stephens, R. Lin, B. Wang, B. Chen, H. V. R. Dias, *Angew. Chem. Int. Ed.* **2021**, *60*, 27184–27188.

[14] A. Noonikara-Poyil, A. Munoz-Castro, A. Boretskyi, P. K. Mykhailiuk, H. V. R. Dias, *Chem. Sci.* **2021**, *12*, 14618–14623.

[15] a) P. J. Perez, M. Brookhart, J. L. Templeton, *Organometallics* **1993**, *12*, 261–262; b) J. M. Munoz-Molina, T. R. Belderrain, P. J. Perez, *Coord. Chem. Rev.* **2019**, *390*, 171–189.

[16] K. Fujisawa, Y. Noguchi, Y. Miyashita, K.-i. Okamoto, N. Lehnert, *Inorg. Chem.* **2007**, *46*, 10607–10623.

[17] A. Boni, G. Pampaloni, R. Peloso, D. Belletti, C. Graiff, A. Tiripicchio, *J. Organomet. Chem.* **2006**, *691*, 5602–5609.

[18] G. Pampaloni, R. Peloso, D. Belletti, C. Graiff, A. Tiripicchio, *Organometallics* **2007**, *26*, 4278–4286.

[19] R. A. Peralta, M. T. Huxley, J. Albalad, C. J. Sumby, C. J. Doonan, *Inorg. Chem.* **2021**, *60*, 11775–11783.

[20] a) C.-C. Chou, H.-J. Liu, C.-C. Su, *Dalton Trans.* **2008**, 3358–3362; b) C.-C. Chou, C.-C. Su, H.-L. Tsai, K.-H. Lii, *Inorg. Chem.* **2005**, *44*, 628–632.

[21] a) I. Bassanetti, M. Mattarozzi, M. Delferro, T. J. Marks, L. Marchiò, *Eur. J. Inorg. Chem.* **2016**, *2016*, 2626–2633; b) M. José Calhorda, P. J. Costa, O. Crespo, M. C. Gimeno, P. G. Jones, A. Laguna, M. Naranjo, S. Quintal, Y.-J. Shi, M. D. Villacampa, *Dalton Trans.* **2006**, 4104–4113; c) K. Fujisawa, R. Kanda, Y. Miyashita, K.-i. Okamoto, *Polyhedron* **2008**, *27*, 1432–1446.
[22] a) Y.-C. Lin, D. Sundholm, J. Jusélius, L.-F. Cui, X. Li, H.-J. Zhai, L.-S. Wang, *J. Phys. Chem. A* **2006**, *110*, 4244–4250; b) A. C. Tsipis, *Organometallics* **2010**, *29*, 354–363; c) J. Jover, F. Maseras, *J. Org. Chem.* **2014**, *79*, 11981–11987; d) M. Besora, A. A. C. Braga, W. M. C. Sameera, J. Urbano, M. R. Fructos, P. J. Pérez, F. Maseras, *J. Organomet. Chem.* **2015**, *784*, 2–12.
[23] P. Motloch, J. Jašík, J. Roithová, *Organometallics* **2021**, *40*, 1492–1502.
[24] L. Jašíková, J. Roithová, *Organometallics* **2012**, *31*, 1935–1942.
[25] a) M. Fianchini, C. F. Campana, B. Chilukuri, T. R. Cundari, V. Petricek, H. V. R. Dias, *Organometallics* **2013**, *32*, 3034–3041; b) H. V. R. Dias, M. Fianchini, T. R. Cundari, C. F. Campana, *Angew. Chem. Int. Ed.* **2008**, *47*, 556–559; *Angew. Chem.* **2008**, *120*, 566–569.
[26] M. Fianchini, H. Dai, H. V. R. Dias, *Chem. Commun.* **2009**, 6373–6375.
[27] K. Klimovica, K. Kirschbaum, O. Daugulis, *Organometallics* **2016**, *35*, 2938–2943.
[28] a) H. V. R. Dias, J. Wu, *Organometallics* **2012**, *31*, 1511–1517; b) H. V. R. Dias, J. Wu, *Eur. J. Inorg. Chem.* **2008**, 509–522.
[29] a) R. S. Nyholm, *Proc. Chem. Soc.* **1961**, 273–296; b) C. Elschenbroich, *Organometallics, 3rd, Completely Revised and Extended Edition*, 3rd ed., Wiley, Weinheim, **2006**.
[30] a) P. O. Oguadinma, F. Schaper, *Organometallics* **2009**, *28*, 6721–6731; b) T. F. van Dijkman, M. A. Siegler, E. Bouwman, *Dalton Trans.* **2015**, *44*, 21109–21123; c) M. Munakata, S. Kitagawa, S. Kosome, A. Asahara, *Inorg. Chem.* **1986**, *25*, 2622–2627; d) A. B. Kazi, H. V. R. Dias, S. M. Tekarli, G. R. Morello, T. R. Cundari, *Organometallics* **2009**, *28*, 1826–1831.
[31] a) G. Santiso-Quiñones, A. Reisinger, J. Slattery, I. Krossing, *Chem. Commun.* **2007**, 5046–5048; b) I. Krossing, A. Reisinger, *Angew. Chem. Int. Ed.* **2003**, *42*, 5725–5728; *Angew. Chem.* **2003**, *115*, 5903–5906; c) J. Schaefer, D. Himmel, I. Krossing, *Eur. J. Inorg. Chem.* **2013**, *2013*, 2712–2717.
[32] Y. Liu, C. Chen, H. Li, K.-W. Huang, J. Tan, Z. Weng, *Organometallics* **2013**, *32*, 6587–6592.
[33] D. J. Gulliver, W. Levason, M. Webster, *Inorg. Chim. Acta* **1981**, *52*, 153–159.
[34] a) A. Bayler, A. Schier, G. A. Bowmaker, H. Schmidbaur, *J. Am. Chem. Soc.* **1996**, *118*, 7006–7007; b) M. A. Omary, M. A. Rawashdeh-Omary, M. W. A. Gonser, O. Elbjeirami, T. Grimes, T. R. Cundari, H. V. K. Diyabalanage, C. S. P. Gamage, H. V. R. Dias, *Inorg. Chem.* **2005**, *44*, 8200–8210.
[35] a) J. S. Thompson, J. F. Whitney, *Inorg. Chem.* **1984**, *23*, 2813–2819; b) J. J. Allen, A. R. Barron, *J. Chem. Crystallogr.* **2009**, *39*, 935; c) J. J. Allen, A. R. Barron, *Dalton Trans.* **2009**, 878–890.
[36] a) N. C. Craig, P. Groner, D. C. McKean, *J. Phys. Chem. A* **2006**, *110*, 7461–7469; b) G. J. H. van Nes, F. van Bolhuis, *Acta Crystallogr. Sect. B* **1979**, *35*, 2580–2593.
[37] S. G. Ridlen, J. Wu, N. V. Kulkarni, H. V. R. Dias, *Eur. J. Inorg. Chem.* **2016**, 2573–2580.
[38] A. Reisinger, N. Trapp, C. Knapp, D. Himmel, F. Breher, H. Rüegger, I. Krossing, *Chem. Eur. J.* **2009**, *15*, 9505–9520.
[39] C. R. Groom, I. J. Bruno, M. P. Lightfoot, S. C. Ward, *Acta Crystallogr. Sect. B* **2016**, *72*, 171–179.
[40] H. V. R. Dias, J. A. Flores, J. Wu, P. Kroll, *J. Am. Chem. Soc.* **2009**, *131*, 11249–11255.
[41] T. J. Brown, R. A. Widenhoefer, *J. Organomet. Chem.* **2011**, *696*, 1216–1220.
[42] J. Wu, A. Noonikara-Poyil, A. Munoz-Castro, H. V. R. Dias, *Chem. Commun.* **2021**, *57*, 978–981.
[43] NIST Chemistry WebBook, SRD 69, Gas Phase IR Spectrum of 1-Pentyne. https://webbook.nist.gov/cgi/cbook.cgi?ID=C627190&Units=SI&Mask=80#Refs (accessed 8/25/2021).
[44] a) J. B. Geri, N. C. Pernicone, J. T. York, *Polyhedron* **2013**, *52*, 207–215; b) G. Jana, S. Pan, P. K. Chattaraj, *J. Phys. Chem. A* **2017**, *121*, 3803–3817.
[45] M. S. Nechaev, V. M. Rayón, G. Frenking, *J. Phys. Chem. A* **2004**, *108*, 3134–3142.
[46] a) H.-C. Tai, I. Krossing, M. Seth, D. V. Deubel, *Organometallics* **2004**, *23*, 2343–2349; b) M. Pernpointner, A. S. K. Hashmi, *J. Chem. Theory Comput.* **2009**, *5*, 2717–2725.
[47] C. Lepetit, V. Maraval, Y. Canac, R. Chauvin, *Coord. Chem. Rev.* **2016**, *308*, 59–75.

Manuscript received: November 4, 2021
Accepted manuscript online: January 24, 2022
Version of record online: February 8, 2022